Int. J. Heat Mass Transfer. Vol. 27, No. 8, pp. 1319–1325, 1984
Printed in Great Britain

0017–9310/84 $3.00 + 0.00
© 1984 Pergamon Press Ltd.

NON-CONDENSABLE GAS EFFECT ON CONDENSATION IN A TWO-PHASE CLOSED THERMOSYPHON

K. HIJIKATA, S. J. CHEN and C. L. TIEN

Department of Mechanical Engineering, University of California, Berkeley, CA 94720, U.S.A.

(*Received* 11 *July* 1983 *and in revised form* 25 *October* 1983)

Abstract—An analytical study is made of the non-condensable gas effect on vapor condensation in a two-phase closed thermosyphon. Particular attention is given to the retardation of vapor condensation due to both radial and axial mass diffusion of gas. The present two-dimensional analysis indicates the inadequacy of the common one-dimensional diffuse-front model in considering only the axial diffusion of gas. The parametric study on radial diffusion shows that the significance of this effect is governed by two dimensionless factors: the gas load and the ratio of the radial gas diffusion rate to the vapor condensation rate.

NOMENCLATURE

D	mass diffusivity
E	radial diffusion parameter, $\rho_s D h_{fg}/[h_c(T_s - T_b)R]$
F	transformed mass fraction, $E \ln \omega_g$
h_c	heat transfer coefficient from wall to coolant
h_{fg}	latent heat of vapor
k_l	thermal conductivity of liquid
L_g	gas-load length, $M_g/(\rho_s \pi R^2)$
L_g^*	dimensionless gas-load length, L_g/R
L_{off}	shut-off condenser length
L_{off}^*	dimensionless shut-off condenser length, L_{off}/R
$\dot{\mathbf{m}}_g$	mass flux vector of gas
M_g	total gas mass
P_s	saturation pressure
r	radial coordinate
r^*	dimensionless radial coordinate, r/R
R	radius of pipe
T_b	bulk temperature of coolant
T_i	interfacial temperature
T_s	saturation temperature
T_w	wall temperature
T_*	characteristic temperature
u	r-component velocity
$\mathbf{V}$	mixture velocity vector
v	z-component velocity
z	axial coordinate
z^*	dimensionless axial coordinate, z/R.

Greek symbols

δ	liquid film thickness
θ	dimensionless temperature, $(T_i - T_b)/(T_s - T_b)$
θ_b	dimensionless temperature, $(T_i - T_b)/(T_s - T_b)$
ρ_g	gas density
ρ_l	liquid density
ρ_s	saturation density
ρ_{vi}	vapor density at interface
ω_g	mass fraction of gas.

1. INTRODUCTION

A TWO-phase closed thermosyphon is basically a gravity-assisted wickless heat pipe. Vapor generated by heating the working liquid rises up the tube and condenses in the condenser region; the condensate returns to the evaporator section by gravity as the falling film [1, 2]. One common troublesome problem in the performance of a heat pipe is the presence of non-condensable gas which may come from system leaks, dissolved gas in the working fluid, and/or adsorbed gas in the pipe structure. Unlike the vertical-plate condensation problem [3, 4], the non-condensable gas is swept along with the vapor flow and accumulates at the condenser end of the pipe forming a gas plug [5, 6]. This plug represents a diffusion barrier to the flowing vapor and almost completely shuts off that portion of the condenser. Indeed a small amount of gas may shut down the operation of a heat pipe, particularly at low pressures.

Despite this detrimental effect, the presence of non-condensable gas can also be utilized in a positive manner to help control the system temperature. A feature which makes it attractive [6] is that the heat pipe accomplishes this temperature control passively through variation in condenser area. With the increase in the operating temperature, the vapor pressure of the working fluid increases, thus compressing the non-condensable gas into a smaller volume and providing a greater active condenser area. The converse operation is similar. With proper design, the gas-controlled heat pipe becomes a constant-temperature variable-conductance device, which has received considerable attention [6].

Because of these important detrimental as well as positive features, the effect of non-condensable gas on heat pipe performance has been studied analytically and experimentally [6]. An earlier method to analyze this effect was based on the flat-front model which assumes a sharp interface between the active and shut-off portions. An improved model assumes the one-dimensional (1-D) diffuse front [6, 7]. This assumption is not entirely satisfactory, since in addition to axial mass diffusion, radial diffusion causes gas to accumulate at the vapor–liquid interface, thus retarding vapor condensation. Rohani and Tien [8] solved numerically the steady two-dimensional (2-D) mass, momentum, heat and species conservation equations in the vapor–gas region of a gas-loaded heat

pipe. Their results demonstrate that energy and mass transfer between vapor and gas may indeed play a dominant role in determining the system performance, however, the simplifying assumptions in their boundary conditions are not quite justified.

The present work establishes a 2-D model to analyze the gas effect on condensation in a two-phase closed thermosyphon. Three specific cases are examined and presented using water as the working fluid. It is demonstrated that mass diffusion between vapor and gas in the radial direction may have an appreciable effect on the heat transfer in the vapor–gas region and on the temperature distribution along the condenser wall. In this regard, the common 1-D diffuse-front model is inadequate to describe the operational characteristics of a gas-loaded thermosyphon, particularly when only small amounts of gas are present.

2. PHYSICAL MODEL AND FORMULATIONS

On account of the rather complicated flow field in a thermosyphon under realistic operating conditions, an idealized 2-D diffusion model was chosen to achieve an understanding of the non-condensable gas effect on condensation. The physical model consists of a condenser with pure saturated vapor flowing vertically upward from the evaporator as shown schematically in Fig. 1. The cylindrical coordinates (r, z) have their origin chosen to coincide with the center of the insulated top end-cap and the corresponding velocity components are (u, v). The system pressure P_s is assumed to be uniform and the incoming pure vapor is at the corresponding saturation temperature T_s. The temperature at the interface of the liquid and the vapor–gas mixture is denoted by T_i and the wall temperature by T_w. Coolant flows outside the condenser tube at bulk temperature T_b and the heat transfer coefficient h_c from the wall to the coolant is constant. In this analysis, heat conduction in the wall is neglected, realizing the wall thickness being very small in most actual systems. The vapor–gas mixture is assumed to follow the ideal gas law. Since $(T_s - T_b)/T_s$ is small, the mixture density ρ_s is assumed to be uniform at the corresponding saturated vapor density of P_s, thus allowing the effect of the buoyancy force on the gas motion to be neglected.

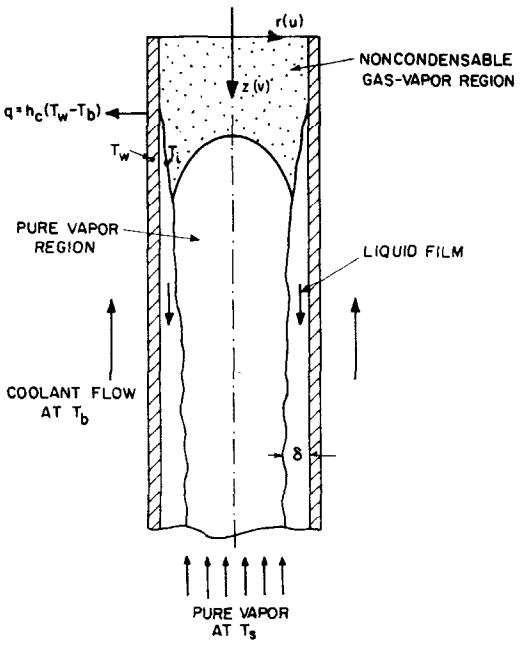

FIG. 1. Schematic of the condenser in a two-phase closed thermosyphon.

After a long period of operation, the non-condensable gas in the system accumulates at the top of the condenser. Since it does not participate in the condensation process, the gas remains stationary. Also, since most of the vapor is condensed in the lower portion of the condenser and the flow rates are small in the region of interest, the mixture flow is laminar and the liquid film follows the Nusselt-type solution. Application of Fick's law of diffusion to the gas mass flow with diffusivity D yields

$$\dot{\mathbf{m}}_g = \rho_g \mathbf{V} - \rho_s D \nabla \omega_g, \tag{1}$$

where $\mathbf{V}$ is the mixture velocity and ω_g is the mass fraction of gas defined by

$$\omega_g = \rho_g / \rho_s. \tag{2}$$

Since $\dot{\mathbf{m}}_g = 0$, equation (1) becomes

$$\mathbf{V} = D \nabla (\ln \omega_g). \tag{3}$$

The continuity equation yields

$$\nabla^2 (\ln \omega_g) = 0, \tag{4}$$

where the mixture density variation has been neglected and the diffusivity is taken to be constant.

The associated boundary conditions, making use of the fact that the liquid film thickness δ is much smaller than the radius R, are

$$\text{at } z = 0: \quad v = 0 \quad \text{or} \quad \partial (\ln \omega_g)/\partial z = 0, \tag{5}$$

$$\text{at } z = \infty: \quad \omega_g = 0, \tag{6}$$

$$\text{at } r = 0: \quad u = 0 \quad \text{or} \quad \partial (\ln \omega_g)/\partial r = 0, \tag{7}$$

$$\text{at } r = R: \quad \omega_g = 1 - (T_s/T_i) \exp [T_*(1 - T_s/T_i)], \tag{8}$$

$$\rho_s D \partial (\ln) \omega_g)/\partial r = h_c (T_i - T_b)/h_{fg}. \tag{9}$$

Equation (8) refers to the saturated vapor at the interface of the liquid film and the mixture flow. It follows from the Clausius–Clapeyron equation that

$$\omega_{gi} = 1 - \rho_{vi}/\rho_s = 1 - (T_s/T_i)(P_{vi}/P_s)$$
$$= 1 - (T_s/T_i) \exp [T_*(1 - T_s/T_i)], \tag{10}$$

where T_* is a function of T_s depending on the material properties.

The last boundary condition, equation (9), can be obtained by referring to Fig. 1. The mass balance at each cross-section, following the Nusselt solution for

the liquid film, gives

$$(g\rho_l^2\delta^2/\mu_l)\,\mathrm{d}\delta/\mathrm{d}z = \rho_s u|_{r=R} = \rho_s D\partial(\ln\omega_g)/\partial r|_{r=R},$$

where the expression on the LHS denotes the amount of condensate added between z and $z+\mathrm{d}z$, and on the RHS, the curvature effect of the interface on the vapor flow is neglected. The energy balance for the film gives

$$k_l(T_i - T_w)/\delta = h_c(T_w - T_b), \tag{11}$$

$$(g\rho_l^2 h_{fg}\delta^2/\mu_l)\,\mathrm{d}\delta/\mathrm{d}z = k_l(T_i - T_w)/\delta. \tag{12}$$

Solving T_w from equation (11) yields

$$T_w = (T_i + h_c\delta T_b/k_l)/(1 + h_c\delta/k_l). \tag{13}$$

However, the liquid film is so thin in this region that it is reasonable to assume that $1+(h_c\delta/k_l)\approx 1$. With this assumption, the above four equations can be combined, resulting in equation (9).

Of the infinitely many solutions of the above equations, only one will satisfy the total gas amount loaded. The amount of non-condensable gas is given as

$$\int_0^\infty\int_0^R \rho_g 2\pi r\,\mathrm{d}r\,\mathrm{d}z = M_g. \tag{14}$$

Dividing by $\rho_s\pi R^2$, it becomes

$$\int_0^\infty\int_0^R \omega_g(r/R)\mathrm{d}(r/R)\,\mathrm{d}z = 0.5L_g, \tag{15}$$

where L_g is the length the gas would occupy if all the gas were restricted to the top of the condenser.

To nondimensionalize the above equations, the following dimensionless quantities are introduced

$$r^* = r/R, \quad z^* = z/R, \quad L_g^* = L_g/R,$$

$$\theta = (T_i - T_b)/(T_s - T_b), \quad \theta_b = T_b/(T_s - T_b),$$

$$E = \rho_s D h_{fg}/[h_c(T_s - T_b)R], \quad F = E\ln\omega_g.$$

The governing equation (4) then becomes

$$(1/r^*)\partial/\partial r^*(r^*\partial F/\partial r^*) + \partial^2 F/\partial z^{*2} = 0, \tag{16}$$

and the boundary conditions, equations (5)–(9), reduce to

$$\text{at } z^* = 0: \quad \partial F/\partial z^* = 0, \tag{17}$$

$$\text{at } z^* = \infty: \quad F = -\infty, \tag{18}$$

$$\text{at } r^* = 0: \quad \partial F/\partial r^* = 0, \tag{19}$$

$$\text{at } r^* = 1: \begin{cases} \exp(F/E) = 1-(1+\theta_b)/(\theta+\theta_b) \\ \qquad\qquad \times\exp[T_*(\theta-1)/(\theta+\theta_b)], & (20) \\ \partial F/\partial r^* = \theta, & (21) \end{cases}$$

with the constraint

$$\int_0^\infty\int_0^1 \exp(F/E) r^*\,\mathrm{d}r^*\,\mathrm{d}z^* = 0.5L_g^*, \tag{22}$$

where the parameter E comes from the vapor condensation rate at the vapor–liquid interface and is the ratio of the gas diffusion rate to the vapor condensation rate.

In contrast with the above interfacial accumulation, the 1-D diffuse-front model assumes a uniform gas concentration at each cross-section [6, 7], and results in the expressions given below.

Governing equations

$$\mathrm{d}^2F/\mathrm{d}z^{*2} = -2\theta, \tag{23}$$

$$\exp(F/E) = 1-(1+\theta_b)/(\theta+\theta_b) \times\exp[T_*(\theta-1)/(\theta+\theta_b)]. \tag{24}$$

Boundary conditions

$$\text{at } z^* = 0: \quad \partial F/\partial z^* = 0, \tag{25}$$

$$\text{at } z^* = \infty: \quad F = -\infty. \tag{26}$$

Constraint

$$\int_0^\infty \exp(F/E)\,\mathrm{d}z^* = L_g^*. \tag{27}$$

3. SOLUTION SCHEME

To avoid the numerical difficulty caused by the unbounded boundary condition, equation (18), the distribution of F at large z^* is obtained from the analytical solution of equation (16). Physically, the gas concentration decreases downward along the condenser, and as it finally vanishes, the pure vapor is saturated at P_s and θ becomes unity. Therefore, by using the method of separation of variables, the solution of equation (16) for large z^* takes the form

$$F = -z^{*2} + (r^{*2}/2) + az^* + b + \sum_{n=1}^{\infty}[C_n\exp(-\alpha_n z^*) + D_n\exp(\alpha_n z^*)]\,J_0(\alpha_n r^*), \tag{28}$$

where a and b are arbitrary constants and J_0 is the zero-order Bessel function. The eigenvalues α_n can be determined from the first-order Bessel function, i.e. $J_1(\alpha_n) = 0$. For solving F at large z^*, the term $\exp(-\alpha_n z^*)$ can be neglected. On the other hand, because of its nature, the $J_0(\alpha_n r^*)$ function alternates for each α_n. It is therefore obvious that D should vanish for regions where the term $\exp(\alpha_n z^*)$ is dominant. Thus, equation (28), for z^* greater than some certain large z_c^*, reduces to

$$F = -z^{*2} + (r^{*2}/2) + C^*(z^*), \tag{29}$$

where $C^*(z^*)$ as a consequence of the numerical solution is defined as

$$C^*(z^*) = az^* + b. \tag{30}$$

It is noted from physical considerations that F is monotonically decreasing with respect to z^*. The expression for F in equation (29) is seen to have a maximum value. The choice of z_c^* which makes equation (29) valid is such that z_c^* is greater than this maximum point.

The central finite-difference scheme is applied to solve the governing equation (16) with the boundary

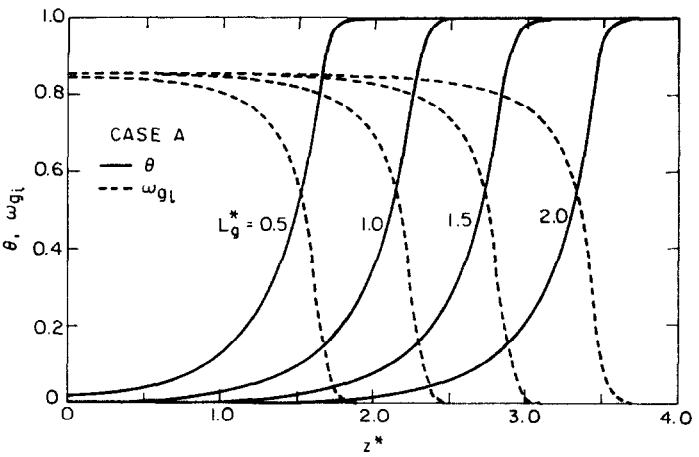

FIG. 2. Interfacial temperature and gas mass fraction distributions based on the 2-D analysis (Case A).

conditions, equations (17)–(21), and the constraint, equation (22). The iteration procedure is as follows: (1) choose a large number for z^*; (2) guess C^* for equation (29); (3) solve θ and F by iteration for this particular C^* starting from an initial guess of θ; (4) integrate exp (F/E) over the whole region; (5) adjust C^* until the constraint, equation (22), is satisfied.

Table 1. Three cases under study ($T_b = 20°C$, $h_c = 800$ W m^{-2} K^{-1})

Case	T_s (°C)	R (cm)	E	θ_b	ρ_s (kg m^{-3})
A	60	1.42	0.0192	7.325	0.14
B	60	2.84	0.0096	7.325	0.14
C	80	1.42	0.0263	4.883	0.29

4. RESULTS AND DISCUSSION

In order to demonstrate the effects of the two parameters E and L_g^*, three cases were examined using steam–air mixtures, as shown in Table 1. The findings from these cases can be applied to other working fluids and similar systems.

The interfacial temperature and gas concentration distributions along the condenser in Case A, as predicted by using the current model, are shown in Fig. 2 for different gas loads, $L_g^* = 0.5$, 1.0, 1.5 and 2.0. For comparison, the distributions calculated from the 1-D diffuse-front model for the same case are plotted in Fig. 3. It is seen that the gas-plug front predicted by the 1-D analysis is still rather sharp. However, the present analysis shows that each profile is shifted to a greater axial distance. As mentioned before, the gas tends to accumulate at the vapor–liquid interface. Consequently, the gas plug spreads and extends along the interface. To see this shift more clearly, the radial distribution of gas concentration is shown in Figs. 4 and 5 for the case being considered. It is seen that in addition to the accumulation near the top end, the gas is also distributed along the interface. Moreover, near the point $z^* = L_g^* + 0.5$, the gas still remains at the interface even though the gas concentration in the region of the mixture-core center nearly vanishes. The effective condenser length for vapor condensation is thus

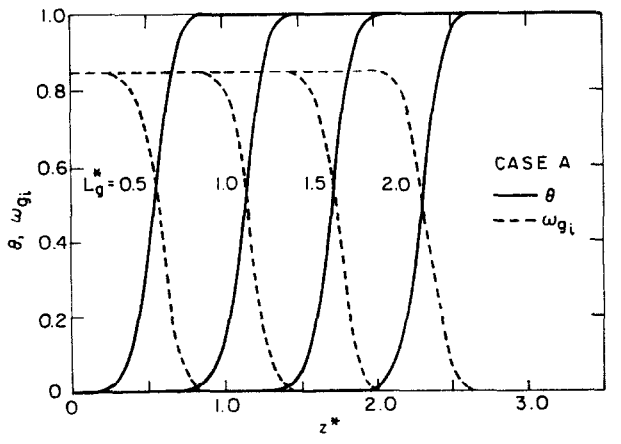

FIG. 3. Interfacial temperature and gas mass fraction distributions based on the 1-D analysis (Case A).

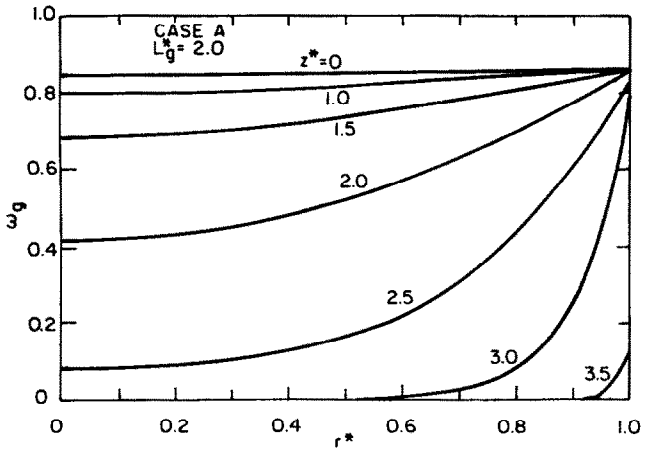

FIG. 4. Radial distribution of gas mass fraction (Case A; $L_g^* = 2.0$).

reduced more than is predicted by the flat-front or the 1-D diffuse-front model.

It is noted that at large L_g^*, say $L_g^* = 2.0$ in Fig. 4, the gas concentration is quite uniform across the mixture core in the region $z^* < L_g^*$. Near the front, $z^* \approx L_g^*$, radial diffusion of gas becomes important. Due to this, the effective condenser length is decreased further by about one radius compared to that calculated from the 1-D analysis.

At smaller L_g^*, radial diffusion of gas is more dominant. Near the top end of the thermosyphon the gas concentration at the core center decreases as the value of L_g^* decreases (see Figs. 4 and 5). For $L_g^* = 0.5$ shown in Fig. 5, the gas concentration at the center is much smaller than that at the interface. As a result, the effective condenser length is relatively further reduced as is seen in Figs. 2 and 3. In fact, at still smaller L_g^*, it is possible to have a gas concentration distribution of the boundary layer type. The gas is mainly concentrated within this layer near the vapor–liquid interface; the asymptotic behavior can be obtained from equation (16) by neglecting the curvature effect and rescaling the length in terms of L_g^*.

Figure 6 shows the dimensionless shut-off condenser length, $L_{off}^* = L_{off}/R$, vs L_g^* for Case A, L_{off} being defined as the location where the dimensionless interfacial temperature begins to become unity. It is seen that the smaller the gas amount, the more important radial diffusion becomes. Also, for small amounts of gas, the increase in L_{off}^* compared to that predicted by 1-D analysis becomes more significant. At large L_g^*, the shut-off condenser length is about one radius greater than that predicted by the 1-D analysis and 1.3 radii greater than that predicted by the flat-front model assuming a sharp interface. This indicates that near the front, radial diffusion is important and in the region away from the front, diffusion is mainly in the axial direction.

Varying the pipe radius causes the value of E, the radial diffusion parameter, to change. In Case B, the pipe radius is doubled thus yielding a value of E which is one half of that in Case A. Figure 7 shows the interfacial

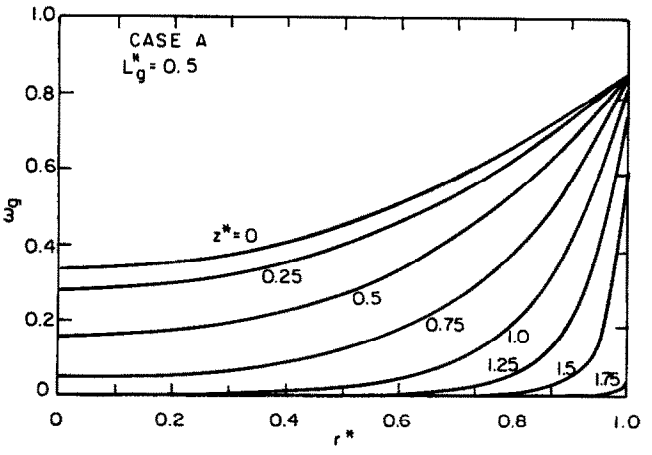

FIG. 5. Radial distribution of gas mass fraction (Case A; $L_g^* = 0.5$).

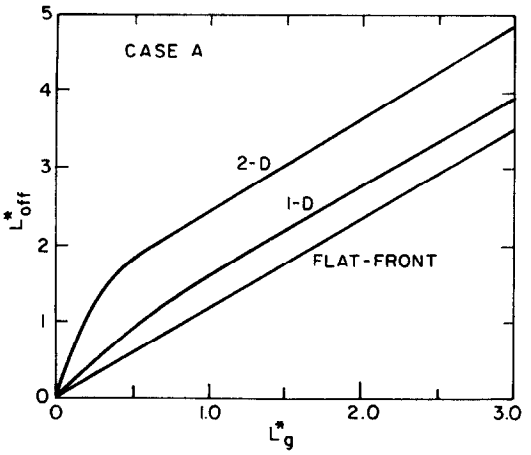

FIG. 6. Shut-off condenser length at different gas amounts loaded (Case A).

temperature and gas concentration distributions along the condenser for Case B. The net effect is to reduce the effective condenser length for a given value of L^*_g. In other words, radial diffusion is more pronounced at smaller values of E. On the other hand, at larger values of E, the problem behaves more like the 1-D diffuse-front model.

The parameter E is also affected by the system operating conditions. At high system pressures, the fixed gas mass is restricted to a small volume. In addition, the parameter E becomes larger due to the increase in the vapor density. The gas-plug effect is thus limited to a smaller region as is shown in Fig. 8 for Case C. It is noted that at a given value of L^*_g, the shut-off condenser length is smaller at this high system pressure than those observed in Figs. 2 and 7.

In view of the above discussion, a general description can be given on the operational characteristics of different working fluids. Large values of E are desirable to minimize the gas effect on vapor condensation. At the same system pressure, the thermosyphon using working fluids which are more volatile, can have larger values of the product, $\rho_s h_{fg}$, and thus the parameter E, although the latent heats of such fluids are relatively lower. In this regard, volatile working fluids are preferred to keep the gas effect at a minimum level. It is, however, noted that the selection of working fluids also depends on the operating temperature range [2].

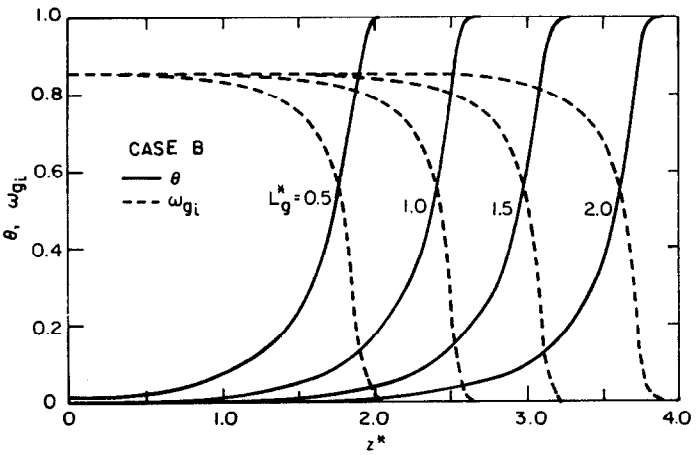

FIG. 7. Interfacial temperature and gas mass fraction distributions based on the 2-D analysis (Case B).

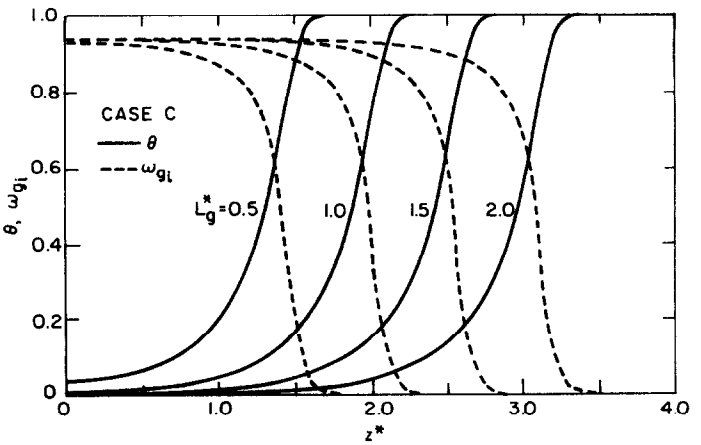

FIG. 8. Interfacial temperature and gas mass fraction distributions based on the 2-D analysis (Case C).

5. CONCLUSIONS

The non-condensable gas effect on vapor condensation in a two-phase closed thermosyphon has been investigated analytically. The results obtained from three cases using steam–air mixtures show that when there is no recirculatory flow, the problem is governed by two dimensionless parameters: the radial diffusion parameter E and the gas load parameter L_g^*. The 1-D diffuse-front model is inadequate to predict the interfacial temperature and thus the shut-off condenser length. At small values of L_g^*, the radial diffusion is increasingly dominant. As a result, the shut-off condenser length is relatively greater. At large values of L_g^*, the gas concentration becomes more uniform across the mixture core except in the region near the front. Radial diffusion near the gas-plug front results in the accumulation of gas at the vapor–liquid interface. It should be noted that due to this accumulation of gas at the interface, the front of the gas plug is shifted further axially and less uniform radially, particularly at small gas loads. The parameter E is related to the vapor condensation rate at the vapor–liquid interface. It indicates the relative importance of radial diffusion. The value of E which incorporates pressure-dependent material properties is also affected by the pipe radius. For a small value of E, radial diffusion is pronounced. At a larger value of E, the problem behaves more like the 1-D diffuse-front model.

Acknowledgements—The authors express their appreciation to the Electric Power Research Institute for the support of this research under Contract EPRI RP 1160-3. Discussions and comments from Dr Jean Pierre Sursock of EPRI were very helpful to the conduct of this work.

REFERENCES

1. T. Fukano, S. J. Chen and C. L. Tien, Operating limits of the closed two-phase thermosyphon, *ASME-JSME Thermal Engineering Joint Conference Proceedings*, Honolulu, Hawaii, Vol. 1, pp. 95–101 (1983).
2. C. L. Tien, Heat pipes, in *Handbook of Heat Transfer*, Chap. 19. McGraw-Hill, New York (1983).
3. E. M. Sparrow and S. H. Lin, Condensation heat transfer in the presence of a non-condensable gas, *J. Heat Transfer* **86**, 430–436 (1964).
4. H. K. Al-Diwany and J. W. Rose, Free convection film condensation of steam in the presence of non-condensing gases, *Int. J. Heat Mass Transfer* **16**, 1359–1369 (1973).
5. Y. Mori, K. Hijikata and K. Utsunomiya, The effect of non-condensable gas on film condensation along a vertical plate in an enclosed chamber, *J. Heat Transfer* **99**, 257–262 (1977).
6. B. D. Marcus, Theory and design of variable conductance heat pipes, NASA Report CR-2018, April (1972).
7. D. K. Edwards and B. D. Marcus, Heat and mass transfer in the vicinity of the vapor–gas front in a gas-loaded heat pipe, *J. Heat Transfer* **94**, 155–162 (1972).
8. A. R. Rohani and C. L. Tien, Steady two-dimensional heat and mass transfer in the vapor–gas region of a gas-loaded heat pipe, *J. Heat Transfer* **95**, 377–382 (1973).

EFFET D'UN GAZ INCONDENSABLE SUR LA CONDENSATION DANS UN THERMOSYPHON FERME ET DIPHASIQUE

Résumé—Une étude analytique porte sur l'effet d'un gaz incondensable sur la condensation d'une vapeur dans un thermosyphon fermé et diphasique. Une attention particulière est portée sur le retard à la condensation dû à la diffusion radiale et axiale du gaz. L'analyse bidimensionnelle indique l'inadéquation du modèle classique monodimensionnel à front de diffusion qui ne considère que la diffusion axiale du gaz. L'étude paramétrique de la diffusion radiale montre que cet effet est gouverné par deux facteurs adimensionnels: la charge de gaz et le rapport du flux de diffusion radial au flux de vapeur condensée.

DER EINFLUSS EINES NICHTKONDENSIERBAREN GASES AUF DIE KONDENSATION IN GESCHLOSSENEN ZWEIPHASEN-THERMOSYPHON

Zusammenfassung—Es wurde eine rechnerische Untersuchung des Einflusses eines nichtkondensierbaren Gases auf die Dampfkondensation in einem geschlossenen Zweiphasen-Thermosyphon durchgeführt. Besonders beachtet wurde die Verschlechterung der Dampfkondensation aufgrund sowohl radialer wie auch axialer Gasdiffusion. Die vorliegende zweidimensionale Untersuchung zeigt die Unzulänglichkeit des üblichen eindimensionalen Diffusionsfrontmodells, das nur axiale Gasdiffusion berücksichtigt. Die parametrische Untersuchung der radialen Diffusion zeigt, daß die Signifikanz dieses Effekts von zwei dimensionslosen Faktoren beherrscht wird: dem Gasgehalt und dem Verhältnis der radialen Gasdiffusionsrate zur Kondensationsrate.

ВЛИЯНИЕ ПРИСУТСТВИЯ НЕКОНДЕНСИРУЮЩЕГОСЯ ГАЗА НА КОНДЕНСАЦИЮ В ДВУХФАЗНОМ ЗАМКНУТОМ ТЕРМОСИФОНЕ

Аннотация—Проведено аналитическое исследование влияния неконденсирующегося газа на конденсацию пара в двухфазном замкнутом термосифоне. Особое внимание обращено на замедление конденсации пара как из-за радиальной, так и аксиальной диффузии массы газа. Проведенный двумерный анализ указывает на неадекватность обычной одномерной модели диффузии, когда рассматривается только аксиальная диффузия газа. Параметрическое исследование радиальной составляющей диффузии показывает, что важность учета этой составляющей определяется двумя безразмерными факторами: весом газа и отношением радиальной скорости диффузии газа к скорости конденсации пара.